Average Field Attenuation in the Nonregular Impedance Street Waveguide

Nathan Blaunstein

***Abstract*— The propagation of electromagnetic (EM) waves in a city with a regularly planned building as a model of a straight street with buildings lining its sides is investigated. The street is considered as a planar two-dimensional (2-D) multislit waveguide with Poisson distributed screens (building walls) and slits (gaps between buildings). The electrical properties of the buildings' walls are taken into account by introducing the electrical impedance as a function of their surface permittivity and conductivity. The average field from the vertical electric dipole placed inside the street lower than rooftop level in the conditions of line-of-sight is investigated using Green's function formalism and real boundary conditions on the building walls. Evaluations show that the total field inside the waveguide can be presented as a superposition of a continuous spectral propagation component, which does not exist in the ideal unbroken waveguide, and a discrete spectral component, which describes the exponential attenuation of reflected and diffracted waves at distances of up to 2–3 km depending on the width of street. The presented model and evaluated formulas are in a good agreement with experimental data of ultrahigh-frequency (UHF)/L-band wave propagation in urban areas with a crossing-street plan.**

***Index Terms*—Land mobile radio propagation factors.**

I. Introduction

THE conditions of electromagnetic (EM) wave propagation in a built-up urban environment are the most difficult of all the types found in ground radio communication because in city areas with regularly planned buildings, multiray reflected and diffracted fields are usually formed leading to significant amplitude and phase variation [1]–[5].

These effects are more apparent in the case of the connection between the base station (radio port) and a stationary or moving object, both located at the street level below the rooftops of buildings. Many experimental and theoretical investigations carried out in city areas show that most of the buildings in built-up regions are practically nontransparent and the total field for ground objects at heights lower than roof level is formed mainly by radio waves reflected from walls and diffracted from corners [5]–[8]. In this case, wide shadow regions with sharp transitions to illuminated zones with laminated interference pictures are observed [9]–[12].

In general, the main influence on field formation in city areas with dense building arises from the local building plan [3], [6], [13]. This is the reason why the processes of radio wave propagation in the city with built-up areas are not described by general statistical [2], [14] or empirical (see bibliography, [15]) models. For the given case, acceptable results can be obtained only for specific circumstances and for particular features of city region planning [3], [6]–[8].

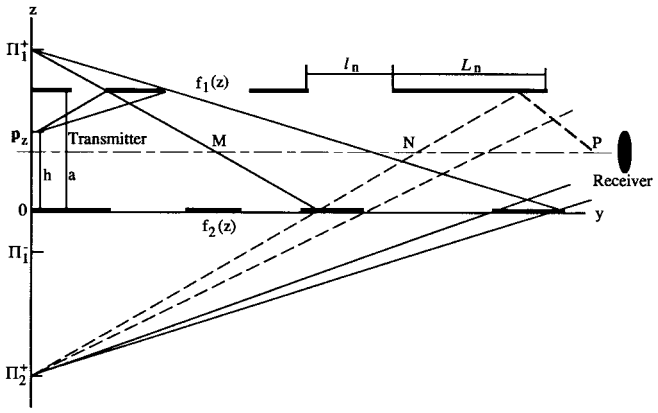

Fig. 1. Ray tracing geometry of the street waveguide and locations of the image sources.

In this work, we investigate the case of EM wave propagation in a city with regular crossing street planning when both objects, receiver and transmitter, are lower than rooftop level. In Section II, the initial conditions of a nonregular multislit waveguide model are presented. Section III describes the total field construction in an impedance plate unbroken waveguide. Section IV presents the method of construction of the wave fields n-times reflected from the broken waveguide screens. In Section V, the procedure of averaging the total field in a nonregular multislit impedance waveguide, using the direct and inverse Fourier transforms for an average total field are examined. The discrete and continuous spectra of the total field are investigated.

Comparisons with results obtained from previously constructed models of ideal conductive broken and unbroken waveguides, as well as with experimental data obtained from the first Tadiran experiments in the urban and suburban environment are presented.

II. The Waveguide Model

The impedance plane parallel waveguide with randomly distributed screens is considered as a model of a city street (see Fig. 1). One waveguide plane is placed at waveguide side $z = 0$, and the second one at $z = a$. The screen L_n and slit l_n lengths are distributed according to the Poisson law with the

Manuscript received March 1, 1996; revised July 1, 1998.

The author is with the Ben-Gurion University of the Negev, Beer-Sheva, 84105 Israel.

Publisher Item Identifier S 0018-926X(98)09681-1.

average values of L and l, respectively

$$L^{-1}\exp\left\{-\frac{L_n}{L}\right\}, \qquad 1^{-1}\exp\left\{-\frac{l_n}{l}\right\}. \tag{1}$$

Let us assume that a vertical electric dipole as a source of EM waves is placed at the point (0, 0, h) on the z axis, where $0 < h < a$ (Fig. 1). The propagation of EM waves is observed at the point inside the waveguide at the image surface (dotted line in Fig. 1).

The real electrical properties of screens (walls) are determined by the surface impedance $Z_{\mathrm{EM}} \sim \varepsilon^{-(1/2)}$, $\varepsilon = \varepsilon_0 - i(4\pi\sigma/\omega)$, where ε is the dielectric permittivity of the wall's surface, ε_0 is the dielectric constant of vacuum, σ is the electric conductivity, and ω is the angular frequency of the radiated wave. Using the harmonic time-dependence $\sim\exp(-i\omega t)$ and the definition of the dipole field using the Hertzian potential vector $\prod_z^i(x, y, z)$, we obtain the well-known equation [16], [17]

$$\nabla^2\prod_z^i - k^2\prod_z^i = -\frac{4\pi i}{\omega}\,\mathbf{p}_z\delta(x)\delta(y)\delta(z-h) \tag{2}$$

the solution of which can be presented using Green's function

$$\prod_z^i(x, y, z) = -\frac{4\pi i}{\omega}\,\mathbf{p}_z\,\frac{e^{ikR}}{R}. \tag{3}$$

Here, $\mathbf{p}_z$ is the electric momentum of a point vertical electric dipole $R = |\mathbf{r}|$, $\mathbf{r}$ is a distance from the source. In real city built-up conditions, the screen and slit lengths are much greater than the radiation wavelength λ, i.e., $L_n \gg \lambda$, $l_n \gg \lambda$. In this case, we can use the approximations of the geometrical theory of diffraction (GTD) first introduced by Keller for the problems of diffraction at the half-plane and wedge [18]. According to the GTD the reflected and diffracted waves have same nature, and the total field can be presented as a superposition of direct wave fields from the source and reflected fields from the screens. Moreover, following the previously constructed model [19], we consider the resulting reflected fields as a sum of the fields reaching the observer from the virtual image sources $\prod_n^+$ (for the reflections from plate $z = a$) and $\prod_n^-$ (for the reflections from plate $z = 0$) (see Fig. 1).

III. Total Field in an Impedance Unbroken Waveguide

As is well known [16], [17], the secondary (reflected) field in an unbroken waveguide can be determined from the wave equation for the Hertzian potential vector

$$\nabla^2\prod_z^r(x, y, z) + k^2\prod_z^r(x, y, z) = 0. \tag{4}$$

Multiplying (4) by the factor $\exp\{-i\alpha x - i\beta y\}$ and using the Fourier transformation of (4), we finally obtain the equation for the Fourier-transformant $\prod_z^r(\alpha, \beta, z)$

$$\left[\frac{\partial^2}{\partial z^2} + (k^2 - \alpha^2 - \beta^2)\right]\prod_z^r(\alpha, \beta, z) = 0 \tag{5}$$

the solution of which can be presented in well known form

$$\prod_z^r(\alpha, \beta, z) = A(\alpha, \beta)\exp\{-iKz\} \tag{6}$$

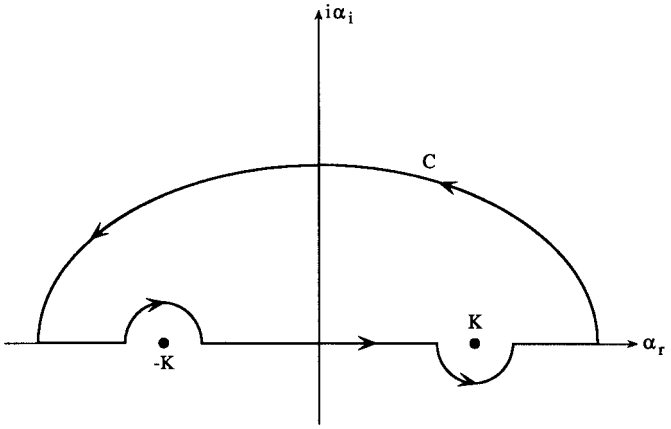

Fig. 2. The integration contour along the semicircle C around the pole points $\alpha_{1,2} = \pm K$.

where $K^2 = k^2 - \alpha^2 - \beta^2$, k is the wave number, and $k = 2\pi/\lambda$. Using the inverse Fourier transform we can obtain the reflected field as

$$\prod_z^r(x, y, z) = \frac{1}{(2\pi)^2}\iint_{-\infty}^{+\infty} A(\alpha, \beta)e^{-iKz - i\alpha x - i\beta y}\,d\alpha\,d\beta. \tag{7}$$

The first (incident from the source) field can be calculated using the direct Fourier transform of free-space Green's function (3)

$$\prod_z^i(\alpha, \beta, \gamma) = -\frac{4\pi i}{\omega}\,\mathbf{p}_z\,\frac{e^{i\gamma h}}{k^2 - \alpha^2 - \beta^2 - \gamma^2} \tag{8}$$

and the inverse Fourier transform with variable γ; we finally obtain the following expression:

$$\begin{aligned}\prod_z^i(\alpha, \beta, z) &= -\frac{4\pi i\mathbf{p}_z}{2\pi\omega}\int_{-\infty}^{\infty}\frac{e^{-i\gamma(z-h)}}{K^2 - \gamma^2} \\ &= \frac{\mathbf{D}}{2\pi}\int_C\frac{e^{-i\gamma(z-h)}}{K^2 - \gamma^2}.\end{aligned} \tag{9}$$

Here, an integral along the semicircular contour C around the pole branch points $\gamma_1 = +K$ and $\gamma_2 = -K$ is introduced in Fig. 2. Using Cauchy's theorem for the branch points, we finally obtain the expression for the Hertzian source potential vector

$$\prod_z^i(\alpha, \beta, z) = \begin{cases}\dfrac{\mathbf{D}}{2iK}\,e^{iK(z-h)}, & z < h \\ \dfrac{\mathbf{D}}{2iK}\,e^{-iK(z-h)}, & z < h\end{cases} \tag{10}$$

where $\mathbf{D}$ is a constant vector, $\mathbf{D} = -(4\pi i/\omega)\mathbf{p}_z$. Now the field from the source (first field) can be presented as

$$\begin{aligned}&\prod_z^i(x, y, z) \\ &\quad= \frac{1}{(2\pi)^2}\iint_{-\infty}^{+\infty}\prod(\alpha, \beta)e^{\pm iK(z-h) - i\alpha x - i\beta y}\,d\alpha\,d\beta\end{aligned} \tag{11}$$

where sign "+" corresponds to $z > h$ sign "−" to $z < h$.

The total field in the unbroken waveguide can be rewritten in the following form:

$$\prod_z(x, y, z) = \frac{1}{2\pi^2}\int A(\alpha, \beta)e^{-iKz-i\alpha x-i\beta y}\,d\alpha\,d\beta + \frac{1}{(2\pi)^2}\int\int \prod(\alpha, \beta)e^{\pm iK(z-h)-i\alpha x-i\beta y}\,d\alpha\,d\beta. \quad (12)$$

Here, as can be seen from (10), $\prod(\alpha, \beta) = D/2iK$; $A(\alpha, \beta)$ is determined from boundary conditions $D = |\mathbf{D}|$. Let us now evaluate the boundary conditions in the impedance-unbroken waveguide.

Using the well-known boundary condition [16], [17]

$$E_y = Z_{\mathrm{EM}}H_x; \qquad E_x = -Z_{\mathrm{EM}}H_y \quad (13)$$

and the relation between the electric and magnetic fields of an EM wave and the Hertzian vector [16], [17], we finally obtain at the boundaries $z = 0$ and $z = a$, respectively

for plate $z = 0$

$$\frac{\partial\prod_z}{\partial z} + ikZ_{\mathrm{EM}}\prod_z = 0 \quad (14)$$

from which

$$A(\alpha, \beta) = \frac{K + kZ_{\mathrm{EM}}}{K - kZ_{\mathrm{EM}}}\,\frac{1}{2iK} = \frac{R_1}{2iK} \quad (15)$$

and for plate $z = a$

$$-\frac{\partial\prod_z}{\partial z} + ikZ_{\mathrm{EM}}\prod_z = 0 \quad (16)$$

from which

$$A(\alpha, \beta) = \frac{K - kZ_{\mathrm{EM}}}{K + kZ_{\mathrm{EM}}}\cdot\frac{e^{2iKa}}{2iK} = \frac{R_2e^{i2Ka}}{2iK}. \quad (17)$$

Finally, the total field in the impedance-unbroken waveguide can be presented as

for $z = 0$

$$\prod_z(x, y, z) = \frac{1}{(2\pi)^2}\iint R_1\prod(\alpha, \beta)e^{-iKz-i\alpha x-i\beta y}\,d\alpha\,d\beta + \frac{1}{(2\pi)^2}\iint \prod(\alpha, \beta)e^{-iK(z-h)-i\alpha x-i\beta y}\,d\alpha\,d\beta \quad (18a)$$

for $z = a$

$$\prod_z(x, y, z) = \frac{1}{(2\pi)^2}\iint R_2\prod(\alpha, \beta)e^{iK(z+2a)-i\alpha x-i\beta y}\,d\alpha\,d\beta + \frac{1}{(2\pi)^2}\iint \prod(\alpha, \beta)e^{iK(z-h)-i\alpha x-i\beta y}\,d\alpha\,d\beta. \quad (18b)$$

We shall use (10) and (18) for the construction of the average field in the discrete multislit waveguide.

IV. EM Waves n-Times Reflected from the Screens in a Broken Waveguide

Here we assume that screens (walls) and slits (gaps between buildings) are distributed according to the Poisson law [see (1)]. Reflection from screens and their corners is taken into account by introducing the special "telegraph signal" functions $f_1(y)$ and $f_2(y)$ defined for the first and the second waveguide walls, respectively, as [19]

$$f_{1,2}(y) = \begin{cases} 1, & \text{on the screen} \\ 0, & \text{on the slit.} \end{cases} \quad (19)$$

Next, we introduce the image sources as presented in Fig. 1 and denote them for the first reflection from surface $z = a$ by the symbol "+" and for the first reflection from surface $z = 0$ the symbol "−." In first stage, we construct the reflected wave fields when the first reflection takes place from the waveguide wall $z = a$. From geometrical construction we define $r_1 = [(a-h)^2 + y_1^2]^{1/2}$; $y_1 = y_M(a-h)/(2a-h-z)$ from which we have a new calculated argument y_1 for the function f_1. Thus, the first wave field reflected from the plate $z = a$ at the point M on the image surface inside the waveguide and along the z axis is

$$\prod\nolimits_{z_1}^{+} \sim \frac{e^{ikr_1}}{r_1}\,f_1\left[\frac{(a-h)y_M}{2a-h-z}\right]. \quad (20)$$

Using the same geometrical considerations for the second reflection from the wall $z = 0$ (the image source $\prod_2^+$) in the derivation of $r_2 = [(2a-h)^2 + y_2^2]^{1/2}$, $y_2 = y_N(2a-h)/(2a-h+z)$, we obtain for the twice-reflected field at the point N inside the waveguide along the z axis

$$\prod\nolimits_{z_2}^{+} \sim \frac{e^{ikr_2}}{r_2}\,f_1\left[\frac{(a-h)y_N}{2a-h+z}\right]f_2\left[\frac{(2a-h)y_N}{2a-h+z}\right]. \quad (21)$$

After the third reflection from the upper plate $z = a$ we obtain at point P for the function f_1 a new argument $y_3 = y_P(3a-h)/(4a-h-z)$, $r_3 = [(3a-h)^2 + y_3^2]^{1/2}$, and the contribution from the third image source $\prod_{z_3}^+$ is

$$\prod\nolimits_{z_3}^{+} \sim \frac{e^{ikr_3}}{r_3}\,f_1\left[\frac{(a-h)y_P}{4a-h-z}\right]f_2\left[\frac{(2a-h)y_P}{4a-h-z}\right] \times f_1\left[\frac{(3a-h)y_P}{4a-h-z}\right]. \quad (22)$$

Following the same procedure by the induction method, we obtain for the n-time reflected wave field when the first reflection taken place from the plate $z = a$, the following:

for even $n = 2m$, $m = 1, 2, 3, \cdots$

$$\prod\nolimits_{z_n}^{+} \sim \frac{e^{ikr_n}}{r_n}\,f_1\left[\frac{(a-h)y}{na-h+z}\right]f_2\left[\frac{(2a-h)y}{na-h+z}\right] \times\cdots\times f_1\left[\frac{((n-1)a-h)y}{na-h+z}\right]f_2\left[\frac{(na-h)y}{na-h+z}\right] \quad (23a)$$

for odd $n = 2m+1,\ m = 1, 2, 3, \cdots$

$$\prod\nolimits^{+}_{z_n} \sim \frac{e^{ikr_n}}{r_n} f_1\left[\frac{(a-h)y}{(n+1)a-h-z}\right] f_2\left[\frac{(2a-h)y}{(n+1)a-h-z}\right] \times \cdots \times f_2\left[\frac{((n-1)a-h)y}{(n+1)a-h-z}\right] \times f_1\left[\frac{(na-h)y}{(n+1)a-h-z}\right]. \quad (23b)$$

The same procedure can be used for the first reflection taking place from the second waveguide wall $z = 0$, i.e., for the image sources $\prod^{-}_{n}$ (see Fig. 1). After similar geometric consideration we obtain the following:

for even $n = 2m,\ m = 1, 2, 3, \cdots$

$$\prod\nolimits^{-}_{z_n} \sim \frac{e^{ikr'_n}}{r'_n} f_2\left[\frac{hy}{na+h-z}\right] f_1\left[\frac{(a+h)y}{na+h-z}\right] \times \cdots \times f_2\left[\frac{((n-2)a+h)y}{na+h-z}\right] f_1\left[\frac{((n-1)a+h)y}{na+h-z}\right] \quad (24a)$$

for odd $n = 2m+1,\ m = 1, 2, 3, \cdots$

$$\prod\nolimits^{-}_{z_n} \sim \frac{e^{ikr'_n}}{r'_n} f_2\left[\frac{hy}{(n-1)a+h+z}\right] f_1\left[\frac{(a+h)y}{(n-1)a+h+z}\right] \times \cdots \times f_1\left[\frac{((n-2)a+h)y}{(n-1)a+h+z}\right] \times f_2\left[\frac{((n-1)a+h)y}{(n-1)a+h+z}\right]. \quad (24b)$$

V. The Average Field in the Impedance Multislit Waveguide

As was shown in [19], the statistical moments of the reflected field inside the multislit waveguide relate to the statistical moments of "telegraph signal" functions $f_1(y)$ and $f_2(y)$ defined by (19) using the procedure

$$\langle f_i(y)\rangle = \chi = \frac{L}{L+l}, \qquad i = 1, 2 \quad (25a)$$

$$\langle f_i(y_1) f_i(y_2)\rangle = \chi^2 K(y_1 - y_2) \quad (25b)$$

$$\langle f_i(y_1) f_i(y_2) f_i(y_3)\rangle = \chi^3 K(y_1 - y_2) K(y_2 - y_3) \quad (25c)$$

and

$$\langle f_i(y_1) f_i(y_2) \cdots f_i(y_2)\rangle = \chi^n \prod\nolimits_{\nu=1}^{n-1} K(y_{\nu-1} - y_\nu) \quad (25d)$$

where $K(w)$ is the correlation function of the "telegraph" signal functions

$$K(w) = \chi^2\left\{1 + \frac{1}{L}\exp\left[-\left(\frac{1}{L}+\frac{1}{l}\right)|w|\right]\right\}. \quad (26)$$

Taking into account the fact that the slit and screen distributions in the street waveguide are statistically independent, i.e.,

$$\langle f_1(y) f_2(y)\rangle = \langle f_1(y)\rangle \langle f_2(y)\rangle = \chi^2 \quad (27)$$

and using the relationships (25a)–(25c), we derived for the n-times reflected fields the expression as a sum of two terms. The first one describes the average reflected field inside the waveguide when first reflection was from the wall $z = a$

$$\left\langle \prod\nolimits^{+}_{z_n} \right\rangle = \frac{e^{ikr_n}}{r_n} \chi^n R^n \prod(\alpha, \beta) e^{iK((n+1)a-z-h)} \times K^{n-2}\left(\frac{2ay}{(n+1)a-z-h}\right), \quad n = 2m+1,\ m = 1, 2, 3, \cdots \quad (28a)$$

$$\left\langle \prod\nolimits^{+}_{z_n} \right\rangle = \frac{e^{ikr_n}}{r_n} \chi^n R^n \prod(\alpha, \beta) e^{iK(na+z-h)} \times K^{n-2}\left(\frac{2ay}{na+z-h}\right), \quad n = 2m,\ m = 1, 2, 3, \cdots. \quad (28b)$$

The second term describes the average reflected field inside the waveguide when the first reflection was from the wall $z = 0$:

$$\left\langle \prod\nolimits^{-}_{z_n} \right\rangle = \frac{e^{ikr'_n}}{r'_n} \chi^n R^n \prod(\alpha, \beta) e^{iK((n-1)a+z+h)} \times K^{n-2}\left(\frac{2ay}{(n-1)a+z+h}\right), \quad n = 2m+1,\ m = 1, 2, 3, \cdots \quad (29a)$$

$$\left\langle \prod\nolimits^{-}_{z_n} \right\rangle = \frac{e^{ikr'_n}}{r'_n} \chi^n R^n \prod(\alpha, \beta) e^{iK(na-z+h)} \times K^{n-2}\left(\frac{2ay}{na-z+h}\right), \quad n = 2m,\ m = 1, 2, 3, \cdots. \quad (29b)$$

Here $R = (K - kZ_{\mathrm{EM}})/(K + kZ_{\mathrm{EM}})$ is the coefficient of reflections from the impedance walls.

As was shown in [19], in (28) and (29) with great accuracy, the condition of $K^{n-2}(Z) \approx 1$ can be assumed.

Using this fact and after some straightforward calculations, we can present the spatial spectrum of an average n-time reflected field in the following form:

$$\prod(\alpha, \beta, z) = \frac{D}{2iK}\left\{\left[\frac{\chi^2 R^2 e^{iK(2a-h)} + \chi R e^{iKh}}{1 - \chi^2 R^2 e^{i2Ka}}\right] e^{iKz} + \left[\frac{\chi^2 R^2 e^{iKh} + \chi R e^{-iKh}}{1 - \chi^2 R^2 e^{i2Ka}}\right] e^{iK(2a-z)}\right\}. \quad (30)$$

Using the inverse Fourier transform for the second (reflected) field (30) and the direct field transformation

for $z < h$

$$\prod\nolimits^{i}_{z}(\alpha, \beta, z) = \prod(\alpha, \beta) e^{-iK(z-h)} \quad (31a)$$

for $z > h$

$$\prod\nolimits^{i}_{z}(\alpha, \beta, z) = \prod(\alpha, \beta) e^{iK(z-h)} \quad (31b)$$

we obtain the same integrals as in (18), which now describes

the total field in the broken multislit waveguide

for $z < h$

$$\prod_z(x, y, z) = \frac{1}{(2\pi)^2} \iint_{-\infty}^{+\infty} d\alpha\, d\beta\, \frac{D}{2iK}\, e^{-i\alpha x - i\beta y} \times \left\{ \left[\frac{\chi R(\chi R e^{iK(2a-h)} + e^{iKh})}{1 - \chi^2 R^2 e^{i2Ka}} \right] e^{iKz} + \left[\frac{\chi R e^{iK(2a-h)} + e^{iKh}}{1 - \chi^2 R^2 e^{i2Ka}} \right] e^{-iKz} \right\} \tag{32a}$$

for $z > h$

$$\prod_z(x, y, z) = \frac{1}{(2\pi)^2} \iint_{-\infty}^{+\infty} d\alpha\, d\beta\, \frac{D}{2iK}\, e^{-i\alpha x - i\beta y} \times \left\{ \left[\frac{\chi R(\chi R e^{iK(2a+h)} + e^{iK(2a-h)})}{1 - \chi^2 R^2 e^{i2Ka}} \right] e^{-iKz} + \left[\frac{\chi R e^{iKh} + e^{-iKh}}{1 - \chi^2 R^2 e^{i2Ka}} \right] e^{iKz} \right\}. \tag{32b}$$

To evaluate these integrals, we introduce the polar coordinate system: $\alpha = \rho \cos \varphi, \beta = \rho \sin \varphi, x = r \cos \psi, y = r \sin \psi$, and take into account the following form of the Bessel function $J_0(z)$ representation [20]:

$$J_0(\rho r) = \frac{1}{2\pi} \int_{0+\psi}^{2\pi+\psi} e^{-i\rho r \cos w}\, dw.$$

Now, taking into account the relationship between the Bessel function $J_0(z)$ and the first-order $H_0^{(1)}(z)$ and second-order $H_0^{(2)}(z)$ Hankel functions: $J_0(z) = [H_0^{(1)}(z) + H_0^{(2)}(z)]/2$, we can rewrite the integrals in (32) in the simplified form

$$\prod_z(x, y, z) = \frac{D}{4\pi i} \int_0^{\infty} \frac{\rho F_{1,2}(\rho) H_0^{(1)}(\rho r)}{\sqrt{k^2 - \rho^2}}\, d\rho. \tag{33}$$

Here, $F_1(\rho)$ and $F_2(\rho)$ are the functions in brackets in (32a) and (32b), respectively, where value K is replaced by $\sqrt{k^2 - \rho^2}$. The integrals (33) can be separated into two parts: the integral along the deformed contour C on which the integrand is analytic and the integral along a branch cut contour γ near the poles depicted in Fig. 3. Here, taking into account the requirement for the integrals (33) to be finite, the condition $\operatorname{Im} K > 0$ must be applied, i.e., the contour C must be closed in the upper half-plane as presented in Fig. 3.

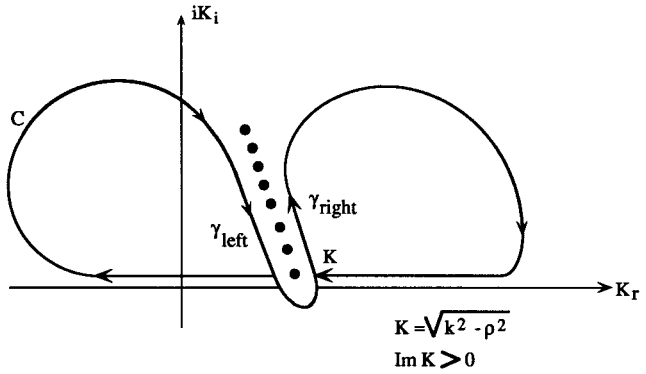

Fig. 3. The deformed contour C in the upper half-plane. The branch-cut contour γ is placed near the poles.

A. The Discrete Spectrum of Total Field

The integral along the closed contour C in the upper half-plane presents the discrete spectrum of the total field inside the multislit waveguide and can be calculated using Cauchy's theorem

$$\oint_C = 2\pi i \sum_{n=0}^{\infty} \operatorname{Res}\left[H_0^{(1)}(\rho r) \rho F_{1,2}(\rho);\ \rho_n \right]. \tag{34}$$

The pole points are determined from

$$1 = \chi^2 R^2 e^{i2ka} = 0$$

from which the pole coordinates are determined

$$\begin{aligned} \rho_n &= (k^2 - K_n^2)^{1/2} \\ K_n &= \pm \frac{\pi n}{a} + i \frac{\ln|\chi|}{a} - \frac{\varphi_n}{a} \\ &= \operatorname{Re} K_n + \operatorname{Im} K_n, \qquad n = 1, 2, 3, \cdots. \end{aligned} \tag{35}$$

Now, the coefficient of reflection of normal modes in the impedance ($Z_{\mathrm{EM}} \neq 0$) multislit waveguide, $R_n = (K_n - kZ_{\mathrm{EM}})/(K_n + kZ_{\mathrm{EM}})$ can be described by use of its phase φ_n and its modules $|R_n|$ presentation as shown in (36) at the bottom of the page. Using formulas (34) and (36), we finally obtain for the discrete spectrum for the case $z > h$

$$\prod_z(x, y, z) = \frac{D}{2a} \frac{H_0^{(1)}(\rho_n r)}{\left[R_n - 2 \dfrac{kZ_{\mathrm{EM}}}{(K_n + kZ_{\mathrm{EM}})^2} \right]} \times \left\{ 2R_n \cos[K_n(z-h)] + \frac{1}{\chi} \left[e^{-iK_n(z+h)} + e^{iK_n(z+h-2a)} \right] \right\} \tag{37a}$$

$$|R_n| = \frac{\sqrt{[(\operatorname{Re} K_n)^2 + (\operatorname{Im} K_n)^2 - (kZ_{\mathrm{EM}})^2]^2 + 4(\operatorname{Im} K_n) Z_{\mathrm{EM}}^2}}{(\operatorname{Re} K_n + kZ_{\mathrm{EM}})^2 + (\operatorname{Im} K_n)^2}$$
$$\varphi_n = \tan^{-1} \frac{2 \operatorname{Im} K_n k Z_{\mathrm{EM}}}{(\operatorname{Re} K_n)^2 + (\operatorname{Im} K_n)^2 - (kZ_{\mathrm{EM}})^2} \tag{36}$$

and for the case $z < h$

$$\prod_z(x, y, z) = \frac{D}{2a} \frac{H_0^{(1)}(\rho_n r)}{\left[R_n - 2\dfrac{kZ_{\rm EM}}{(K_n + kZ_{\rm EM})}\right]} \times \left\{ R_n E^{iK_n(z-h-a)} + e^{-iK_n(z+h+a)} + e^{iK_n(z+h-3a)} + \frac{1}{R_n} e^{-iK_n(z-h+3a)} \right\}. \tag{37b}$$

Each index n in the poles (36) corresponds to a waveguide mode of an average reflected field. It is easy to show that for $r/a \gg 1$, this discrete waveguide mode spectrum can be significantly simplified. Thus for the case $z > h$ we obtain

$$\prod{}^d \approx \frac{C}{\sqrt{r}} \exp(i\rho_n^{(0)} r) \exp\left[-\frac{|\ln \chi R_n|}{\rho_n^{(0)} a} \left(\frac{\pi n - \varphi_n}{a} \right) r \right] \tag{38}$$

where $\rho_n^{(0)} = \sqrt{k^2 - (n\pi/a)^2}$, $C =$ constant.

For the case of an ideal conductive waveguide model, when $Z_{\rm EM} = 0$ and $|R_n| = 1$, $\varphi_n = 0$, we obtain from (37a) and (38) for $z > h$, respectively

$$\prod_z(x, y, z) = \frac{D}{2a} H_0^{(1)}\left(\sqrt{k^2 - K_n^2} r \right) \times \left\{ 2\cos[K_n(z-h)] \frac{1}{\chi} \times \left[e^{-iK_n(z+h)} + e^{iK_n(z+h-2a)} \right] \right\} \tag{39}$$

$$\prod{}^d \approx \frac{C}{\sqrt{r}} \exp(i\rho_n^{(0)} r) \exp\left[-\frac{|\ln \chi|}{\rho_n^{(0)} a} \left(\frac{\pi n}{a} \right) r \right]. \tag{40}$$

These formulas are the same as those obtained for the case of an ideal conductive multislit waveguide and presented for case $z > h$ in [19]. In both waveguides the modes of the discrete spectrum attenuate according to (43) and (45) exponentially inside the broken waveguide and their extinction lengths are given by the following formula:

$$\zeta_n = \frac{\rho_n^{(0)} a}{\left(\dfrac{\pi n - \varphi_n}{a} \right) \ln |\chi R_n|}. \tag{41}$$

The extinction lengths depend on the number of reflections "n," on the waveguide (street) width "a," on the parameter of brokenness χ and on the parameter of wall's surface electric properties R_n. For the case of an unbroken ideal conductive waveguide ($\chi \to 1$, $R_n \to 1$) it follows from (41) that $\zeta_n \to \infty$ and normal modes propagate as waves in an ideal waveguide without attenuation [17]

$$\prod_n \sim \frac{2\pi P_z}{a\omega} \left[H_0^{(1)}(kr) + H_0^{(1)}\left(\sqrt{k^2 - \left(\frac{\pi n}{a}\right)^2} r \right) \times \cos\left(\frac{\pi n h}{a} \right) \cos\left(\frac{\pi n z}{a} \right) \right]. \tag{42}$$

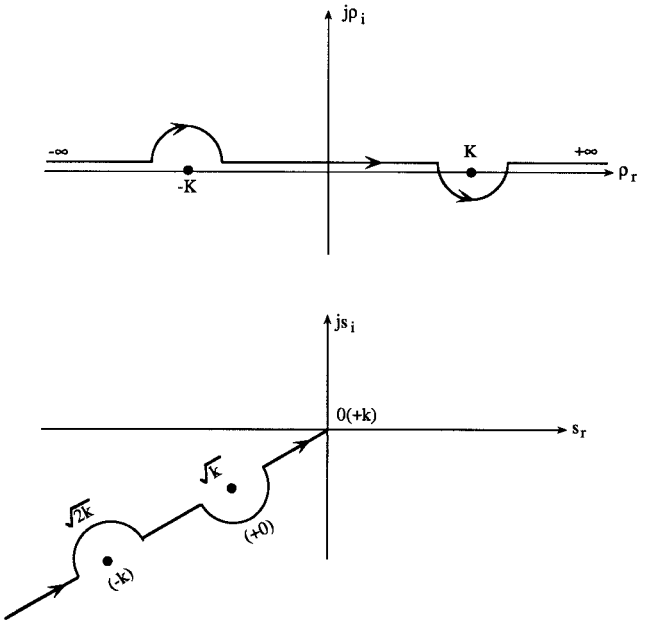

Fig. 4. Transformation from the complex argument ρ to a new complex plane argument s.

In the case of impedance waveguide ($|R_n| \neq 1$) the character of reflected mode attenuation depends on the real values of the electrical impedance $Z_{\rm EM}$. With increasing $Z_{\rm EM}$ ($Z_{\rm EM} > 0$) the extinction lengths becomes smaller and the normal waves in the impedance multislit waveguide attenuate faster than in the case of the ideal conductive multislit waveguide. The same picture is observed with an increase in the number of reflections n: the normal reflected modes in multislit waveguide with numbers $n \geq 5$ attenuate very quickly (corresponding extinction length ζ_n decreases). On the other hand, increasing the value of χ (decreasing the distances between buildings) leads to a decrease of the reflected wave attenuation factor. In the limit of an unbroken waveguide ($\chi = 1$) the normal waves with numbers $n < 5$ (the main reflected modes) also propagate without appreciable (in dependence on parameter $Z_{\rm EM}$) attenuation at large distances.

B. The Continuous Spectrum of Total Field

A continuous spectrum has been evaluated from integration along the contour γ around the branch points (see Fig. 3). We will examine this integral for the case $z > h$, adding it to the source field (31b), which is also found from the contour integral with branch-cut point $\rho = k$

$$\prod{}_z^i = \frac{1}{8\pi} \left(\int_{\gamma\,\rm left} + \int_{\gamma\,\rm right} \right) H_0^{(1)}(\rho r) \frac{iD}{\sqrt{k^2 - \rho^2}} \times e^{i\sqrt{k^2-\rho^2}(z-h)} \rho\, d\rho. \tag{43}$$

Then the continuous part of the total field can be presented as

$$\prod{}_c = \frac{D}{8\pi i} \int_k^{i\infty} \frac{H_0^{(1)}(\rho r)}{\sqrt{k^2 - \rho^2}} Q(z) \rho\, d\rho \tag{44}$$

where

$$Q(z)=\frac{(\chi Re^{iKh}+e^{-iKh})(\chi Re^{iK(2a-z)}+e^{iKz})}{1-\chi^2R^2e^{i2Ka}}+\frac{(\chi Re^{-iKh}+e^{iKh})(\chi Re^{-iK(2a-z)}+e^{-iKz})}{1-\chi^2R^2e^{i2Ka}}. \tag{45}$$

This formula describes the continuous radiation, i.e., average continuous spectrum inside the multislit waveguide. We now transform the integration variables by including a new arguments (see Fig. 4): $\rho = k + is^2$; $d\rho = 2isds$; $s = \exp\{-i3(\pi/4)\}(k-\rho)^{1/2}$. For this argument we have a branch cut point $s = \exp\{i(\pi/4)\}(2k)^{1/2}$ and poles $s^2 = ik \pm (-k^2 + [i \ln \chi|R_n|/a + (n\pi - \varphi_n/a)]^2)^{1/2}$, where $\mathrm{Im}[\exp\{i3(\pi/4)\}(2k+is^2)^{1/2}] > 0$. Using Cauchy's formula for the poles and the asymptotic approximation $H_0(\rho r) \sim (-2i/\pi\rho r)^{1/2}\exp\{i\rho r\}$, we finally derive the continuous spectrum of the total field for $r/a \gg 1$

$$\prod\nolimits_c \approx \sqrt{2}De^{i(3\pi/4)}\frac{1-\chi|R_n|}{1+\chi|R_n|}\frac{e^{ikr}}{4\pi r}. \tag{46}$$

For the case of ideal conductive multislit waveguide when $|R_n| = 1$, $Z_{\mathrm{EM}} = 0$, we can obtain from (46) the same formula presented in [19]. As can be seen from (46) in the broken waveguide the continuous part of the total field propagates as a spherical wave $\sim(e^{ikr}/r)$ and reduces to the unbroken waveguide case in the limit $\chi = 1$. But, if in the ideal conductive unbroken waveguide for the large distances ($r \gg a$) $\prod^c = 0$, in the impedance ideal waveguide with continuous walls the continuous part $\prod^c$ of total field does not vanish because for the case $\chi = 1$ and $|R_n| \neq 1$, $\prod^c$, as can be seen from (46) differs from zero. This is a new principal result which is absent in the case of an ideal conductive waveguide with continuous walls (unbroken).

VI. Contribution to Path Loss

In the impedance unbroken waveguide ($\chi = 1$) the existence of additional term (46) in the case of $Z_{\mathrm{EM}} \neq 0$ ($|R_n| \neq 1$) leads to the additional losses of EM waves propagated inside it. This fact is clearly seen from investigations of path loss. Thus, taking into account the characteristics of a vertical electrical dipole field in free-space and (38) and (46), we can approximately obtain the path loss of radio wave intensity $\sim\langle\prod\cdot\prod^*\rangle$ in an impedance multislit waveguide

$$L \approx 32.1 - 20\log_{10}|R_n| - 20\log_{10}\left[\frac{1-(\chi|R_n|)^2}{1+(\chi|R_n|)^2}\right] + 17.8\log_{10} r + 8.6\cdot\left\{-\ln\chi|R_n|\left[\frac{\pi n-\varphi_n}{a}\right]\frac{r}{\rho_n^{(0)}a}\right\} \tag{47}$$

which, for the case $Z_{\mathrm{EM}} = 0$, $|R_n| = 1$, $\varphi_n = 0$ is the same with path loss estimated for the case of ideal conductive broken waveguide [19].

VII. Comparison with Experimental Data

The measurement were carried out by Tadiran in Kefar Yona, Israel, for the testing the Tadiran Multigain Wireless system as a typical example of local loop system. The tested system operates at the frequencies band $f_0 = 902.5$–927.5 MHz. The tested microcellular built-up area is a typical suburban environment with a crossing-street plan in which the two three-storied buildings (with $h_b = 8$–10 m) are irregularly distributed along the street. The installed radio port (base station) is located near rooftop level ($h_T = 7$ m); the moving receiving antenna is placed below the rooftop level ($h_T = 3$ m). The first experiment was carried out in line-of-sight conditions when receiver and transmitter antennas were placed at the street level with direct visibility and the moving receiver changed its distance from the base station in the range 10–350 m. At the distance $r = 350$ m from the base station the measurements gave

$$L_{\max} = 46 \text{ dB}; \qquad L_{\text{average}} = 43 \text{ dB}; \qquad L_{\min} = 40 \text{ dB}. \tag{48}$$

Estimations from the evaluated formula (47) for the case of mean densely distributed building at the street level ($M = 0.5$) and for street-width $a = 20$ m, range $r = 350$ m, and $f_0 = 902$–928 MHz gave

1) for ferroconcrete building walls with $|R_n| \approx 1$:

$$L = 42.6 \text{ dB}$$

2) for brick building walls with $\varepsilon_0 = 15$–17, $\sigma = 0.05$–0.08 mho/m, $|R_n| \approx 0.73$–0.81:

$$L = 45.3\text{–}46.1 \text{ dB}.$$

VIII. Conclusions

The theoretical model of multislit impedance waveguide constructed above gives a good agreement with experimentally found exponential wave attenuation along streets in the urban and suburban areas up to 1–2 km from the source. This model can be used for the prognosis of ultrahigh-frequency (UHF)/L-band propagation in street-planned urban and suburban microcells having radius less than 1–2 km in the conditions of line-of-sight.

References

[1] F. I. Kegami, S. Yoshida, and M. Takahar, "Analysis of multipath propagation structure in urban mobile radio environments," *IEEE Trans. Antennas Propagat.*, vol. 20, pp. 531–537, May 1980.

[2] G. K. Chan, "Propagation and coverage prediction for cellular radio systems," *IEEE Trans. Veh. Technol.*, vol. 40, pp. 665–670, July 1977.

[3] A. J. Rustako, N. Amitay, G. J. Owens, and R. S. Roman, "Radio propagation at microwave frequencies for line-of-sight microcellular mobile and personal communications," *IEEE Trans. Veh. Technol.*, vol. 40, pp. 203–210, Feb. 1991.

[4] S. T. S. Chia, "Radiowave propagation and handover criteria for microcells," *British Telecom Tech. J.*, vol. 8, pp. 50–61, Oct. 1990.

[5] J. Fumio and J. Susumi, "Analysis of multipath propagation structure in urban mobile radio environments," *IEEE Trans. Antennas Propagat.*, vol. 28, pp. 531–538, May 1980.

[6] J. Walfish and H. L. Bertoni, "A theoretical model of UHF propagation in urban environments," *IEEE Trans. Antennas Propagat.*, vol. 36, pp. 1788–1796, Dec. 1988.

[7] A. J. Levy, "Fine structure of the urban mobile propagation channel," in *Proc. Commsphere* Herzlia, Israel, Oct. 1991, pp. 5.1.1–5.1.6.

[8] S. Y. Tan and H. S. Tan, "UTD propagation model in an urban street scene for microcellular communications," *IEEE Trans. Electromagn. Compat.*, vol. 35, pp. 423–428, Apr. 1993.
[9] K. A. Hughes, "Mobile propagation in London at 936 MHz," *Electron. Letters*, vol. 18, pp. 141–143, Mar. 1982.
[10] R. Y. Samuel, "Mobile radio communications at 920 MHz," in *2nd Int. Conf. Antennas Propagat.*, London, U.K., Apr. 1981, vol. 2, pp. 143–147.
[11] J. H. Whitteker, "Measurements of path loss at 910 MHz for proposed microcell urban mobile systems," *IEEE Trans. Veh. Technol.*, vol. 37, pp. 376–381, Apr. 1988.
[12] P. Harley, "Short distance attenuation measurements at 900 MHz and 1.86 MHz using low antenna heights for microcells," *IEEE Select. Areas Commun.*, vol. 10, pp. 7–16, Feb. 1989.
[13] L. R. Maciel, H. L. Bertoni, and H. H. Xia, "Unified approach to prediction of propagation over buildings for all ranges of base station antenna height," *IEEE Trans. Veh. Technol.*, vol. 42, pp. 41–45, Feb. 1993.
[14] F. I. Kegami, T. Takeuch, and S. Yoshida, "Theoretical prediction of mean field strength for urban mobile radio," *IEEE Trans. Antennas Propagat.*, vol. 39, pp. 299–302, Mar. 1991.
[15] W. C.-Y. Lee, *Mobile Communication Design Fundamentals.* Indianapolis, IN: Sams, 1986.
[16] I. Tolstoy, *Wave Propagation.* New York: McGraw-Hill, 1973.
[17] L. B. Felsen and N. Marcuvitz, *Radiation and Scattering of Waves.* Englewood Cliffs, NY: Prentice-Hall, 1973.
[18] J. B. Keller, "Geometrical theory of diffraction," *J. Opt. Soc. Amer.*, vol. 52, pp. 116–130, Jan. 1962.
[19] N. Blaunshtein and M. Levin, "Prediction of UHF-wave propagation in suburban and rural environments," in *Proc. Commsphere*, Eilat, Israel, Jan. 1995, pp. 191–200.
[20] *Handbook of Mathematical Functions*, M. Abramowitz and I. A. Stegun, Eds. New York: Dover, 1972.

Nathan Blaunstein received the B.Sc. and M.Sc. degrees in radiophysics and electronics from Tomsk University, Tomsk, Russia, in 1972 and 1976, respectively, and the Ph.D. and D.Sc. degrees in radiophysics and electronics from the Institute of Geomagnetism, Ionosphere, and Radiowave Propagation (IZMIR), Academy of Science USSR, Moscow, Russia, in 1985 and 1991, respectively.

From 1993 to 1995, he was a Scientist. Since 1995 was a Senior Scientist of the Department of Electrical and Computer Engineering and a Visiting Professor in the Wireless Cellular Communication program at the Ben-Gurion University of the Negev, Beer-Sheva, Israel. Currently, he is an Associate Professor there. His research interests include problems of radiowave propagation, diffraction, and scattering in various media for purpose of radiolocation, mobile-satellite and terrestrial communications, and for cellular and mobile systems performance and services.